Stem Cell Reports
Report
OPEN ACCESS

Microscale Generation of Cardiospheres Promotes Robust Enrichment of Cardiomyocytes Derived from Human Pluripotent Stem Cells

Doan C. Nguyen,[1,5] Tracy A. Hookway,[2,5] Qingling Wu,[1,2] Rajneesh Jha,[1] Marcela K. Preininger,[1,2] Xuemin Chen,[1] Charles A. Easley,[3] Paul Spearman,[1] Shriprasad R. Deshpande,[1] Kevin Maher,[1] Mary B. Wagner,[1] Todd C. McDevitt,[2,4,*] and Chunhui Xu[1,4,*]

[1]Department of Pediatrics, Emory University School of Medicine and Children's Healthcare of Atlanta, Atlanta, GA 30322, USA
[2]Wallace H. Coulter Department of Biomedical Engineering, Georgia Institute of Technology and Emory University, Atlanta, GA 30332, USA
[3]Department of Cell Biology, Emory University School of Medicine, Atlanta, GA 30322, USA
[4]Parker H. Petit Institute for Bioengineering and Bioscience, Georgia Institute of Technology, Atlanta, GA 30332, USA
[5]Co-first author
*Correspondence: todd.mcdevitt@bme.gatech.edu (T.C.M.), chunhui.xu@emory.edu (C.X.)
http://dx.doi.org/10.1016/j.stemcr.2014.06.002

SUMMARY

Cardiomyocytes derived from human pluripotent stem cells (hPSCs) are a promising cell source for regenerative medicine, disease modeling, and drug discovery, all of which require enriched cardiomyocytes, ideally ones with mature phenotypes. However, current methods are typically performed in 2D environments that produce immature cardiomyocytes within heterogeneous populations. Here, we generated 3D aggregates of cardiomyocytes (cardiospheres) from 2D differentiation cultures of hPSCs using microscale technology and rotary orbital suspension culture. Nearly 100% of the cardiospheres showed spontaneous contractility and synchronous intracellular calcium transients. Strikingly, from starting heterogeneous populations containing ~10%–40% cardiomyocytes, the cell population within the generated cardiospheres featured ~80%–100% cardiomyocytes, corresponding to an enrichment factor of up to 7-fold. Furthermore, cardiomyocytes from cardiospheres exhibited enhanced structural maturation in comparison with those from a parallel 2D culture. Thus, generation of cardiospheres represents a simple and robust method for enrichment of cardiomyocytes in microtissues that have the potential use in regenerative medicine as well as other applications.

INTRODUCTION

Cardiomyocytes (CMs) derived from human pluripotent stem cells (hPSCs) have been found in preclinical studies to prevent the progression of heart failure and function as a biological pacemaker, and therefore are a promising cell source for regenerative medicine to treat cardiovascular diseases (Burridge et al., 2012; Maher and Xu, 2013; Mummery et al., 2012). Extensive engraftment of hPSC-CMs and electromechanical coupling of these cells with the host have been demonstrated in a nonhuman primate model (Chong et al., 2014). An area of great interest to the field of stem cell research is engineering tissue constructs from hPSC-CMs, with the aim of providing better transplantable constructs for regenerative cardiac therapy as well as in vitro models to study human cardiac development, health, and disease. Many current approaches often require a great deal of effort to prepare enriched CMs from differentiation cultures; for example, CMs can be enriched by a mitochondrial dye (Hattori et al., 2010) or metabolic selection (Tohyama et al., 2013) and then aggregated, or by fluorescence-activated cell sorting based on surface markers for the generation of tissue patches (Zhang et al., 2013). Genetically modified hPSCs have also been used to select cardiac progenitors or CMs for the production of tissue-engineered cardiac constructs (Emmert et al., 2013; Thavandiran et al., 2013).

Several strategies to generate tissue-engineered cardiac constructs have been considered, including the self-assembly of 3D cell aggregates. Such aggregates offer several advantages and can be easily generated by forced aggregation and maintained in a rotary orbital suspension culture (Kinney et al., 2011). Microscale technologies allow for the generation of size-controlled 3D multicellular aggregates (Khademhosseini et al., 2006) that can promote cell-cell and cell-matrix interactions analogous to those observed among cells in vivo, which cannot be achieved in traditional 2D cultures. Furthermore, in contrast to macrotissue constructs, microtissue constructs can obviate limitations of oxygen and nutrient transport, do not require additional matrix or scaffold materials, and are suitable for scale-up suspension production, and thus represent a robust method for cardiac tissue engineering (Kinney et al., 2014). Therefore, we produced and characterized scaffold-free 3D cardiospheres from 2D differentiation cultures of hPSCs using microscale technologies. The combined technique of forced aggregation and 3D suspension culture is capable of robustly and rapidly enriching CMs from heterogeneous differentiation cultures, and also promotes enhanced structural maturation of CMs compared with parallel 2D cultures.

RESULTS

Derivation of Human Induced PSC Lines and CM Differentiation

We generated 3D cardiospheres using two human induced pluripotent stem cell (iPSC) lines, 903-19 and 903-20, derived from human dermal fibroblasts (Figure S1 available online); the IMR90 iPSC line (Yu et al., 2007); and the H7 human embryonic stem cell (hESC) line (Thomson et al., 1998). The generated iPSCs expressed PSC markers and generated cell types of all three germ layers (Figure S1), indicating that the 903-19 and 903-20 lines were bona fide PSC lines that might be used for subsequent CM differentiation.

To induce CM differentiation in 2D cultures of the four hPSC lines, the cells were sequentially treated with activin A and BMP4 (Laflamme et al., 2007) or small molecules targeting the Wnt pathway (Lian et al., 2012). In general, spontaneously beating clusters were first observed between days 7 and 9, and gradually increased in number over time. By day 14, cells across large regions of the cultures were strongly contracting (Movie S1) and continued to beat vigorously until they were harvested.

Generation of Uniform Cardiospheres via Microscale Forced Aggregation and Suspension Culture

To produce cardiospheres, 2D differentiation cultures were dissociated and seeded into microwells (Figure 1A). After 24 hr, cell aggregates were transferred to suspension culture and maintained for 7 days. The cells consistently aggregated to form 3D cardiospheres regardless of the initial CM differentiation efficiency (~10%–40%). After 2 days and for the duration of the suspension culture, ~100% of the resulting cardiospheres exhibited spontaneous beating (Movie S2). The cardiospheres maintained their starting size for the entire suspension culture period (Figures 1B and 1C). Histological analysis indicated that the cardiospheres consisted of densely packed cells that were entrapped with relatively little collagen and glycosaminoglycans and lacked visible necrotic centers (Figure 1D), in contrast to the necrotic regions that are often observed in large (>600 μm in diameter) multicellular aggregates of PSCs (Gerecht-Nir et al., 2004).

We next determined whether the cardiospheres had appropriate calcium-handling properties. When incubated with a calcium indicator dye, Fluo-4, all of the cardiospheres showed calcium impulses (Movie S3). Optical recordings of intracellular calcium transients by line scans reflected appropriate cyclic calcium handling (Figure 1E). The average spontaneous beating frequency for these cells was 0.49 Hz, which was in the range reported in the literature for functional hESC-CMs (Lundy et al., 2013), and the amplitude was also consistent with what has been measured in human cardiac cells (Wagner et al., 2005). Other measured parameters, including times to 50% peak and to 50% decay, were also representative of a cardiac-type phenotype. In addition, increased spontaneous beating rates were observed when cells were treated with isoproterenol, a β-adrenergic agonist, indicating an appropriate pharmacological response (Figure 1F).

Altogether, these results suggest that the combination of microscale forced aggregation and suspension culture enables the reliable generation of cardiospheres that retain appropriate calcium handling properties and pharmacological response.

Robust Enrichment of CMs via Cardiosphere Formation

The gross distribution of CMs within cardiospheres was examined by whole-mount staining. Sarcomeric α-actinin$^+$ cells were observed throughout cardiospheres, and punctate connexin 43 staining was seen between the cells within the constructs (Figure 2A). These staining patterns indicated that the majority of the cells in the aggregates were CMs. To further evaluate whether enrichment of CMs occurred in cardiospheres, the proportion of CMs in dissociated cardiospheres was compared with that in parallel 2D cultures by immunocytochemical analysis of α-actinin. Staining of cells from cardiospheres indicated that α-actinin$^+$ cells were abundantly present, with only rare instances of unstained cells (Figure 2B, bottom). In contrast, the majority of cells in 2D cultures lacked α-actinin expression (Figure 2B, top). These results demonstrated that CMs had been greatly enriched from 2D cultures.

To quantify the enrichment efficiency, flow-cytometric analysis was used to determine the percentages of α-actinin$^+$ cells in cardiospheres and parallel 2D cultures. As depicted in Figures 2C and 2D, the percentage of α-actinin$^+$ cells from 3D cultures was enriched to ~90% from ~40%, and to ~80% from ~10%, respectively, from parallel monolayer cultures, translating to an enrichment factor of ~2- to 7-fold. This finding indicated that cardiosphere culture enabled robust enrichment of hPSC-CMs, irrespective of the initial differentiation efficiency of the starting population.

Role of Cell Aggregation in CM Enrichment

To understand the process of CM enrichment and determine when the enrichment primarily occurred, we analyzed the CM purity of cardiospheres and parallel 2D cultures at several time points: before (day 14) and immediately after aggregation (day 14+1) and after 3 or 7 days in suspension culture (day 14+3 and day 14+7, respectively). An input cell population from a 2D culture of H7 cells containing ~30% α-actinin$^+$ cells at day 14 was forced to aggregate into 3D cardiospheres. Compared with parallel 2D

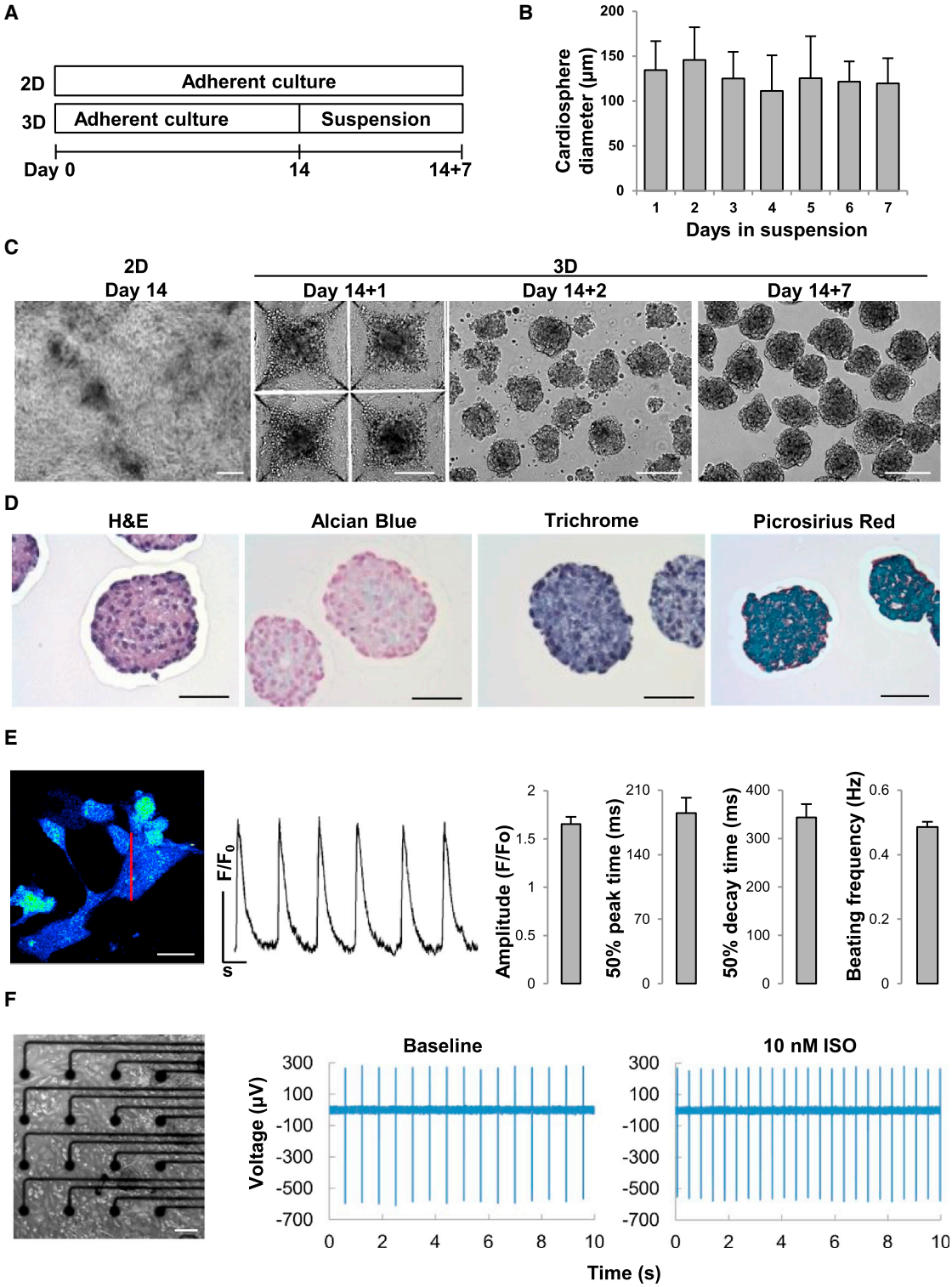

Figure 1. CM Differentiation on Monolayers and Engineering of 3D Cardiospheres

(A) Schematic outlining the procedures used to differentiate hPSCs to CMs in 2D culture and to engineer 3D cardiospheres from 2D cultures.

(B) Size distribution (mean ± SD; n = 11–56 cardiospheres for each time point) of cardiospheres during suspension culture.

(C) Phase-contrast images of CMs generated on monolayers on day 14 postinduction (2D; left), cells 1 day after seeding in microwells (3D; day 14+1), and cardiospheres on day 2 (3D; day 14+2) and day 7 (3D; day 14+7) in suspension. Scale bars represent 200 μm.

(legend continued on next page)

controls, which maintained similar levels of purity during 1 week of adherent culture, the CMs in cardiospheres increased to ~60% 1 day after initiation of cell aggregation (day 14+1), and further increased to ~90% by 3 and 7 days in suspension (days 14+3 and 14+7, respectively; Figure 3A). Therefore, CM enrichment occurred early after initial aggregation and increased further during the subsequent suspension culture phase.

Since enrichment of CMs occurred 1 day after initiation of aggregation, this process was monitored more closely. An input 2D culture containing ~20% α-actinin$^+$ cells with ~90% viability (measured by trypan blue exclusion) was used to form cardiospheres (Figure S2). After 24 hr, a subset of the cells incorporated into cardiospheres while the rest of the cells remained as single cells or small clusters in the supernatant. With input cells at 1,500 cells/microwell, each cardiosphere contained ~600 cells after 1 day of cardiosphere formation, suggesting that selective cell aggregation occurred during cardiosphere formation.

To evaluate the fate of noncardiac cells, we collected both cells in the supernatant fraction (which are typically removed during medium changes) and cardiospheres, and examined them for cell viability and purity of CMs. Cells in the supernatant were mostly single cells with a poor cell viability (~10%). In contrast, the viability of the cells from dissociated 3D cardiospheres was ~90%. When cells from the supernatant were replated, a majority of the cells remained unattached and the cells that did survive were mostly negative for α-actinin. In contrast, cells from cardiospheres attached well and the percentage of α-actinin$^+$ cells increased from ~20% in the 2D culture to ~60% in cardiospheres (Figure S2). Cell counting indicated that ~20% of the initial input non-CMs were recovered in the cardiospheres, suggesting that the majority of non-CMs were dead and remained in the supernatant. Addition of a ROCK inhibitor during cardiosphere formation did not affect viability or CM enrichment (Figure S2). The dramatic difference in cell viability between cardiospheres and cells in the supernatant was confirmed by Annexin V and propidium iodide (PI) staining (Figure 3B). Cardiospheres consisted of ~90% Annexin V$^-$/PI$^-$ (live) cells; in contrast, cells in the supernatant consisted of only ~20% live cells. These results suggest that CMs can preferentially survive and form cardiospheres, whereas the majority of the unincorporated non-CMs do not.

To examine whether the size of the cardiospheres affected enrichment, we formed aggregates of 500, 1,000, or 1,500 input cells/microwell by varying the density of the initial cell suspension (Figure S3A). The input of 500 cells/microwell yielded noticeably smaller aggregates compared with the input of 1,000 or 1,500 cells/microwell. We found that ~97%–100% cells from cardiospheres in all three conditions were positive for α-actinin, whereas only ~14% of the cells from the 2D culture were α-actinin$^+$, suggesting that different seeding densities did not affect the overall enrichment of CMs, but did yield cardiospheres of different sizes (Figure S3B).

Next, we examined whether the proliferation of CMs or conversion from non-CMs (progenitors) into CMs contributed to CM enrichment. Cells from a 2D culture and cardiospheres were costained with antibodies against pH3 (a marker for cells in the proliferative M phase), α-actinin, or NKX2-5 with α-actinin. Only ~2%–4% of pH3$^+$/α-actinin$^+$ cells were detected within the α-actinin$^+$ cells, and ~1%–4% NKX2-5$^+$/α-actinin$^-$ cardiac progenitors were detected, suggesting that proliferation of CMs or conversion from progenitors into CMs was unlikely a major contributor to the enrichment of CMs (Figure S3C). Collectively, these observations suggest that selective cell survival and homophilic adhesion of CMs result in aggregation to form cardiospheres with significant CM enrichment.

To investigate the involvement of specific cell adhesion molecules (N-cadherin and neural cell adhesion molecule-1 [NCAM-1]) in CM aggregation, we incubated dissociated 2D differentiated cultures with antibodies targeting N-cadherin or NCAM-1. At 0 hr, cells in all conditions remained mostly as dissociated single cells. After 4 hr of incubation, we observed large cell aggregates at the center of all wells except those containing perturbing antibodies against NCAM-1, where small cell clusters and single cells were seen throughout the wells. When transferred to flat wells, these aggregates and small clusters maintained their general appearance (Figure 3C). These observations

(D) Histological analysis of cardiospheres after 7 days in suspension culture. Scale bars represent 50 μm.
(E) Calcium transient recordings in live CMs from cardiosphere outgrowths. Left, 2D scans of a cardiosphere outgrowth loaded with Fluo-4, where increasing calcium is indicated by the change in color from dark blue to light green. The red line indicates the location at which the line scan was recorded. Scale bar represents 20 μm. Middle, average calcium intensity along the line scan, with all transients demonstrating cyclic calcium handling. The fluorescence intensity for all recordings is normalized to the baseline measured at time 0 (F_0). Right, summary of the characteristics of calcium transients from cardiosphere outgrowths (mean ± SE; line scans of n = 18 cardiosphere outgrowths).
(F) Pharmacological response of CMs from cardiospheres. The morphology of dissociated cardiospheres in a multielectrode array (MEA) chamber and representative MEA recordings before and after incubation with the β-adrenergic agonist isoproterenol (10 mM) are shown. Note that the beating rate increased upon treatment with isoproterenol. Scale bar represents 100 μm.

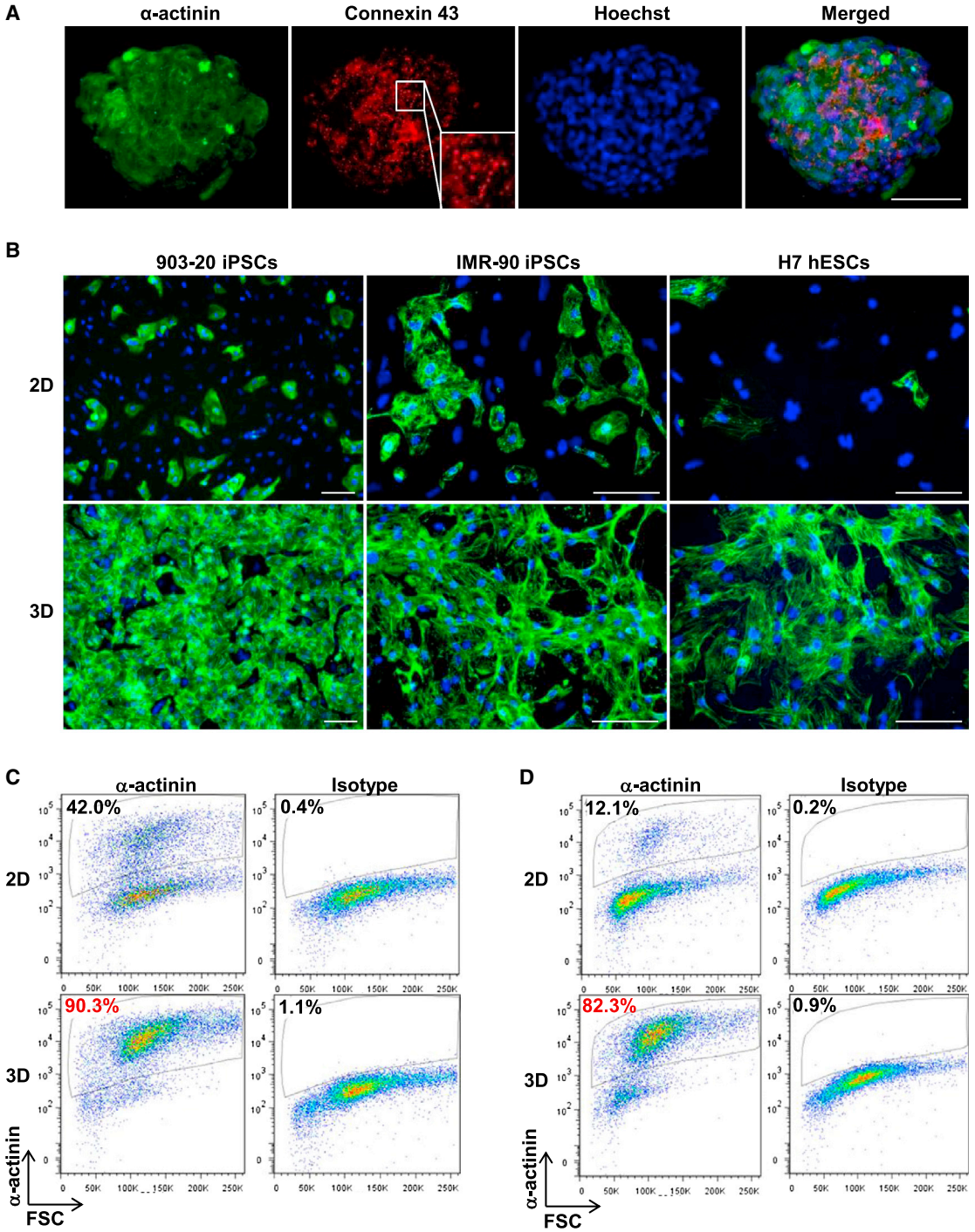

Figure 2. Enrichment of hPSC-CMs via 3D Cardiosphere Culture

(A) Whole-mount staining of 3D cardiospheres for sarcomeric α-actinin and connexin 43. Scale bar represents 50 μm.

(B) Immunostaining for α-actinin of cells harvested from day 21 monolayer cultures (2D; top) and day 7 cardiospheres (3D; bottom) (day 14+7). Dissociated cells from cultures generated from three hPSC lines were immunostained for sarcomeric α-actinin (green) and counterstained for nuclei with DAPI (blue). Scale bars represent 50 μm. Note that α-actinin staining is present throughout the field, with rare occurrences of unstained cells in the samples from 3D cardiospheres.

(legend continued on next page)

implicate NCAM-1 as a likely mediator of CM aggregation into cardiospheres. We next examined whether neuroectoderm cells (which can express NCAM-1) were present in the input 2D cells and 3D cells. SOX2, a stem cell marker that persists in neuroectoderm (Freund et al., 2008), was undetectable in both 2D and 3D cultures, indicating a lack of neuroectoderm cells in the differentiation population. These results suggest that in the absence of neuroectoderm, CMs aggregation is mediated (at least in part) by NCAM-1.

Structural Characteristics and Modulation of Structural Maturation of CMs via Cardiosphere Formation

To examine the microstructure of CMs in cardiospheres, we stained dissociated and replated cardiospheres with cardiac markers, including sarcomeric myosin heavy chain (sMHC), α-actinin, NKX2-5, and cardiac troponin I (cTnI). As shown in Figure 4A, these cells were positive for all of these markers and also featured clear muscle striations when observed under high magnification, suggestive of their bona fide CM status. Next, given the enhanced cell-cell interactions in cardiospheres, we investigated the possible effect of the suspension cultures on CM structural maturity. For this purpose, we compared the z-line sarcomere organization and morphology of CMs that originated from cardiospheres and 2D cultures. More than 200 2D and 3D α-actinin$^+$ CMs were "scored" for their relative levels of z-line sarcomere organization; as such, a cell that received a higher score represented a greater level of sarcomeric structures (Figure 4B). Compared with CMs from 2D cultures, 4.4-fold more cells from 3D cardiospheres exhibited higher levels of sarcomeric striations (level 4 cells), and 1.8- to 5.1-fold fewer cells from 3D cultures showed a morphology of levels 1–3 (Figure 4C). As shown in Figure S4, the sarcomere lengths of the level 4 cells from 3D cultures were significantly higher than those of the level 4 cells from 2D cultures. The length-to-width ratios of α-actinin$^+$ cells in 3D cells were also significantly higher than those in 2D cells, although no significant difference was observed for cell area and cell perimeter (Figure S4). These data suggest that cardiosphere cultures promote several features of structural maturation in hPSC-CMs.

DISCUSSION

Overall, we show that combination of forced aggregation and suspension culture enables the reliable generation of cardiospheres with spontaneous contractility. Strikingly, these cardiospheres contain highly enriched (up to ~100%) CMs that retain expected functional characteristics. The enrichment is particularly robust and efficient irrespective of the starting population, even when cultures contain as little as ~10% CMs. Furthermore, CMs within cardiospheres display enhanced sarcomeric structural maturation compared with those from parallel monolayer cultures. Thus, the use of cardiospheres represents a unique, simple, and straightforward method for the enrichment of CMs. Our findings highlight advantages conferred by 3D tissue engineering of CMs derived from hPSCs.

Enriched CMs are highly desirable for research and translational applications such as drug discovery and cell therapy, as well as mechanistic characterization of inherited cardiac diseases with iPSC-CMs; for example, gene-expression profiling between patient- and unaffected control-specific CMs could be confounded by low CM purity in differentiation cultures. Although efficient CM differentiation methods have been reported (Lian et al., 2012; Zhang et al., 2012), in many cases there remain large variations in CM purity in differentiation cultures, as indeed we experienced in this study even with the well-characterized H7 hESC line. Whereas several techniques allow for the enrichment of CMs from heterogeneous differentiation cultures, such methods nevertheless exist with one or more caveats, such as complex and lengthy procedures, low-to-moderate efficiency, genotoxicity, and/or production of CMs that are labeled with antibodies, dyes, or magnetic beads (Burridge et al., 2012; Xu, 2012). The cardiosphere-mediated enrichment method reported here is simple to perform, is highly efficient, does not require genetic modification, and yields highly enriched CM populations free of any antibodies or dyes. Added benefits of the 3D cardiospheres include potential to overcome challenges of low rates of cell retention following transplantation of dissociated cells and to be directly used for high-throughput in vitro assays in drug discovery.

CM enrichment in cardiospheres is apparently mediated via selective cell survival and homophilic association. NCAM-1 is a cell-surface glycoprotein and calcium-independent adhesion protein that is expressed in developing hearts and other tissues, modulates cell-cell interaction during development (Watanabe, 1998), and was previously found to be highly expressed on hESC-CMs (Xu et al., 2006). This study demonstrates that NCAM-1 plays a functional role in the aggregation of hPSC-CMs. The enrichment of CMs in cardiospheres is likely facilitated

(C) Quantification of CM purity by flow-cytometric analysis for α-actinin on cells derived from 903-20 iPSCs. Numbers indicate the percentage of cells positive for α-actinin (left) or the matching negative isotype control (isotype; right).
(D) Same as (C) except that the 903-20 iPSC line is shown at a later passage. More than 1×10^5 live cells (EMA-negative events) were analyzed in all flow-cytometric analyses.

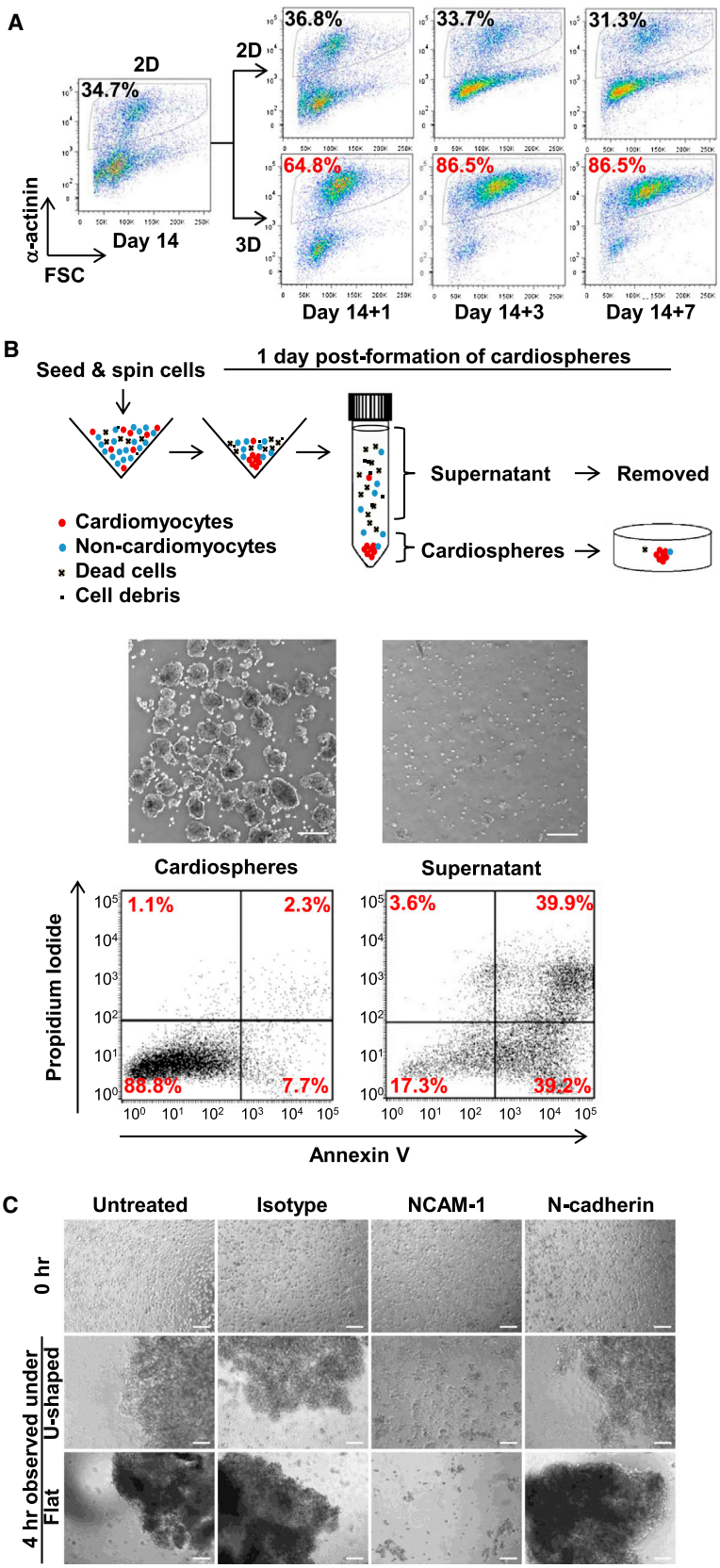

Figure 3. Role of Cell Aggregation in CM Enrichment

(A) Flow-cytometric analysis of α-actinin in H7 2D cultures and 3D cardiospheres at several time points. The purity of CMs was analyzed at day 14, 1 day after initiation of cardiospheres (day 14+1), and after 3 and 7 days in suspension (day 14+3 and day 14+7, respectively). 2D control cultures were analyzed at the same time points. Note that enrichment of CMs was observed soon after initiation of cell aggregation and further in suspension cultures.

(B) Schematic diagram for cardiosphere formation and separation of cells from cardiospheres and supernatant, phase-contrast images, and flow-cytometric analysis of Annexin V and PI in cells from H7 cardiospheres and supernatant on day14+1. Scale bars represent 100 μm.

(C) Cell aggregation inhibition assay. Dissociated differentiation cultures of 903-19 iPSCs were incubated in medium containing the indicated antibodies and monitored at 0 hr or 4 hr after the incubation. Note that the formation of large cell aggregates was prevented in medium containing antibodies against NCAM-1. Scale bars represent 50 μm.

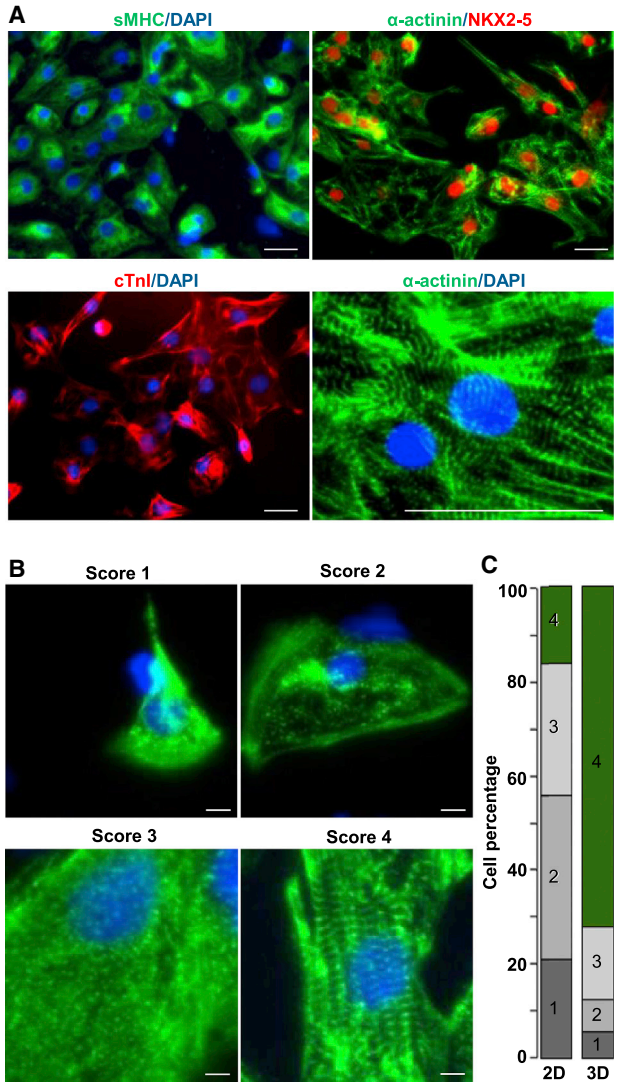

Figure 4. Structural Analysis of CMs from 3D Cardiospheres

(A) Immunocytochemical analysis of cardiac markers on dissociated cardiospheres derived from 903-19 iPSCs. Note that cardiac markers were present throughout the field and that a higher magnification revealed typical cardiac sarcomeric striations. Scale bars represent 50 μm.

(B) Comparison of CM maturation between 2D culture and 3D cardiospheres derived from 903-20 iPSCs. Cardiospheres at day 14+7 and the parallel 2D culture were dissociated, replated, and stained for sarcomeric α-actinin (green) and DAPI (blue). The level of sarcomeric striations was visualized from high-magnification images and given a score of 1–4. Cells that received a score of 1 stained positively for α-actinin, but without clear sarcomeric striations. Cells that were scored 2, 3, or 4 had detectable sarcomeric striations at increasing levels.

(C) Percentage of cells by the scores. Note that cells from 3D cultures displayed higher numbers of cells with more clear sarcomeric striations compared with cells from 2D cultures. Scale bars represent 5 μm.

by a lack of other cell types, such as neuroectoderm that express NCAM-1 in differentiated cultures.

The microscale cardiospheres generated herein exhibit enhanced structural maturation of CMs, suggesting a potential improvement in the utility of tissue-engineered cardiac constructs. This technology also provides a simple and effective method for the enrichment of hPSC-CMs that will be a useful cell source for regenerative therapies and can serve as simple tissue models for drug discovery and development.

EXPERIMENTAL PROCEDURES

Microwell Formation of Cardiospheres

To generate 3D cardiospheres, 2D differentiation cultures on days 14–23 were dissociated with 0.25% trypsin/EDTA and seeded into microwells (Aggrewell 400; StemCell Technologies) at a density of 500–1,500 cells/microwell. After 24 hr, cardiospheres were transferred to rotary orbital suspension culture (at a speed of 60–65 rpm) and maintained for up to 8 days. Upon the completion of culture, cardiospheres were harvested for subsequent characterization.

SUPPLEMENTAL INFORMATION

Supplemental Information includes Supplemental Experimental Procedures, four figures, one table, and three movies and can be found with this article online at http://dx.doi.org/10.1016/j.stemcr.2014.06.002.

AUTHOR CONTRIBUTIONS

C.X. and T.C.M. jointly conceived the study; D.C.N., T.A.H., Q.W., R.J., and M.K.P. performed research; X.C., C.A.E., P.S., S.R.D., K.M., and M.B.W. contributed new reagents and analytic tools; D.C.N., T.A.H., Q.W., R.J., M.K.P., and M.B.W. analyzed data; D.C.N. and C.X. wrote the paper; and T.A.H., M.B.W., and T.C.M. edited the paper.

ACKNOWLEDGMENTS

We thank the staff of the Emory Children's Pediatric Research Flow Cytometry Core for training on flow cytometry. This work was supported in part by the Emory Children's Center (C.X.); the Clinical and Translational Sciences Award Program of the National Center for Advancing Translational Sciences, NIH (PHS grant ULITR00454 to C.X. and T.C.M.); the National Science Foundation (CBET 0939511 to T.C.M.); CASIS (GA-2014-126 to C.X.), and the NIH (R21HL118454 to C.X.). Q.W. and M.K.P. were supported by the Center for Pediatric Nanomedicine under the direction of Dr. Gang Bao.

Received: February 5, 2014
Revised: May 31, 2014
Accepted: June 2, 2014
Published: July 3, 2014

REFERENCES

Burridge, P.W., Keller, G., Gold, J.D., and Wu, J.C. (2012). Production of de novo cardiomyocytes: human pluripotent stem cell differentiation and direct reprogramming. Cell Stem Cell *10*, 16–28.

Chong, J.J., Yang, X., Don, C.W., Minami, E., Liu, Y.W., Weyers, J.J., Mahoney, W.M., Van Biber, B., Palpant, N.J., Gantz, J.A., et al. (2014). Human embryonic-stem-cell-derived cardiomyocytes regenerate non-human primate hearts. Nature. Published online April 30, 2014. http://dx.doi.org/10.1038/nature13233.

Emmert, M.Y., Wolint, P., Wickboldt, N., Gemayel, G., Weber, B., Brokopp, C.E., Boni, A., Falk, V., Bosman, A., Jaconi, M.E., and Hoerstrup, S.P. (2013). Human stem cell-based three-dimensional microtissues for advanced cardiac cell therapies. Biomaterials *34*, 6339–6354.

Freund, C., Ward-van Oostwaard, D., Monshouwer-Kloots, J., van den Brink, S., van Rooijen, M., Xu, X., Zweigerdt, R., Mummery, C., and Passier, R. (2008). Insulin redirects differentiation from cardiogenic mesoderm and endoderm to neuroectoderm in differentiating human embryonic stem cells. Stem Cells *26*, 724–733.

Gerecht-Nir, S., Cohen, S., and Itskovitz-Eldor, J. (2004). Bioreactor cultivation enhances the efficiency of human embryoid body (hEB) formation and differentiation. Biotechnol. Bioeng. *86*, 493–502.

Hattori, F., Chen, H., Yamashita, H., Tohyama, S., Satoh, Y.S., Yuasa, S., Li, W., Yamakawa, H., Tanaka, T., Onitsuka, T., et al. (2010). Nongenetic method for purifying stem cell-derived cardiomyocytes. Nat. Methods *7*, 61–66.

Khademhosseini, A., Langer, R., Borenstein, J., and Vacanti, J.P. (2006). Microscale technologies for tissue engineering and biology. Proc. Natl. Acad. Sci. USA *103*, 2480–2487.

Kinney, M.A., Sargent, C.Y., and McDevitt, T.C. (2011). The multiparametric effects of hydrodynamic environments on stem cell culture. Tissue Eng. Part B Rev. *17*, 249–262.

Kinney, M.A., Hookway, T.A., Wang, Y., and McDevitt, T.C. (2014). Engineering three-dimensional stem cell morphogenesis for the development of tissue models and scalable regenerative therapeutics. Ann. Biomed. Eng. *42*, 352–367.

Laflamme, M.A., Chen, K.Y., Naumova, A.V., Muskheli, V., Fugate, J.A., Dupras, S.K., Reinecke, H., Xu, C., Hassanipour, M., Police, S., et al. (2007). Cardiomyocytes derived from human embryonic stem cells in pro-survival factors enhance function of infarcted rat hearts. Nat. Biotechnol. *25*, 1015–1024.

Lian, X., Hsiao, C., Wilson, G., Zhu, K., Hazeltine, L.B., Azarin, S.M., Raval, K.K., Zhang, J., Kamp, T.J., and Palecek, S.P. (2012). Robust cardiomyocyte differentiation from human pluripotent stem cells via temporal modulation of canonical Wnt signaling. Proc. Natl. Acad. Sci. USA *109*, E1848–E1857.

Lundy, S.D., Zhu, W.Z., Regnier, M., and Laflamme, M.A. (2013). Structural and functional maturation of cardiomyocytes derived from human pluripotent stem cells. Stem Cells Dev. *22*, 1991–2002.

Maher, K.O., and Xu, C. (2013). Marching towards regenerative cardiac therapy with human pluripotent stem cells. Discov. Med. *15*, 349–356.

Mummery, C.L., Zhang, J., Ng, E.S., Elliott, D.A., Elefanty, A.G., and Kamp, T.J. (2012). Differentiation of human embryonic stem cells and induced pluripotent stem cells to cardiomyocytes: a methods overview. Circ. Res. *111*, 344–358.

Thavandiran, N., Dubois, N., Mikryukov, A., Massé, S., Beca, B., Simmons, C.A., Deshpande, V.S., McGarry, J.P., Chen, C.S., Nanthakumar, K., et al. (2013). Design and formulation of functional pluripotent stem cell-derived cardiac microtissues. Proc. Natl. Acad. Sci. USA *110*, E4698–E4707.

Thomson, J.A., Itskovitz-Eldor, J., Shapiro, S.S., Waknitz, M.A., Swiergiel, J.J., Marshall, V.S., and Jones, J.M. (1998). Embryonic stem cell lines derived from human blastocysts. Science *282*, 1145–1147.

Tohyama, S., Hattori, F., Sano, M., Hishiki, T., Nagahata, Y., Matsuura, T., Hashimoto, H., Suzuki, T., Yamashita, H., Satoh, Y., et al. (2013). Distinct metabolic flow enables large-scale purification of mouse and human pluripotent stem cell-derived cardiomyocytes. Cell Stem Cell *12*, 127–137.

Wagner, M.B., Wang, Y., Kumar, R., Tipparaju, S.M., and Joyner, R.W. (2005). Calcium transients in infant human atrial myocytes. Pediatr. Res. *57*, 28–34.

Watanabe, M. (1998). The neural cell adhesion molecule and heart development: what is NCAM doing in the heart? Basic Appl. Myol. *8*, 277–291.

Xu, C. (2012). Differentiation and enrichment of cardiomyocytes from human pluripotent stem cells. J. Mol. Cell. Cardiol. *52*, 1203–1212.

Xu, C., Police, S., Hassanipour, M., and Gold, J.D. (2006). Cardiac bodies: a novel culture method for enrichment of cardiomyocytes derived from human embryonic stem cells. Stem Cells Dev. *15*, 631–639.

Yu, J., Vodyanik, M.A., Smuga-Otto, K., Antosiewicz-Bourget, J., Frane, J.L., Tian, S., Nie, J., Jonsdottir, G.A., Ruotti, V., Stewart, R., et al. (2007). Induced pluripotent stem cell lines derived from human somatic cells. Science *318*, 1917–1920.

Zhang, J., Klos, M., Wilson, G.F., Herman, A.M., Lian, X., Raval, K.K., Barron, M.R., Hou, L., Soerens, A.G., Yu, J., et al. (2012). Extracellular matrix promotes highly efficient cardiac differentiation of human pluripotent stem cells: the matrix sandwich method. Circ. Res. *111*, 1125–1136.

Zhang, D., Shadrin, I.Y., Lam, J., Xian, H.Q., Snodgrass, H.R., and Bursac, N. (2013). Tissue-engineered cardiac patch for advanced functional maturation of human ESC-derived cardiomyocytes. Biomaterials *34*, 5813–5820.

Stem Cell Reports, Volume *3*

Supplemental Information

Microscale Generation of Cardiospheres Promotes Robust Enrichment of Cardiomyocytes Derived from Human Pluripotent Stem Cells

Doan C. Nguyen, Tracy A. Hookway, Qingling Wu, Rajneesh Jha, Marcela K. Preininger, Xuemin Chen, Charles A. Easley, Paul Spearman, Shriprasad R. Deshpande, Kevin Maher, Mary B. Wagner, Todd C. McDevitt, and Chunhui Xu

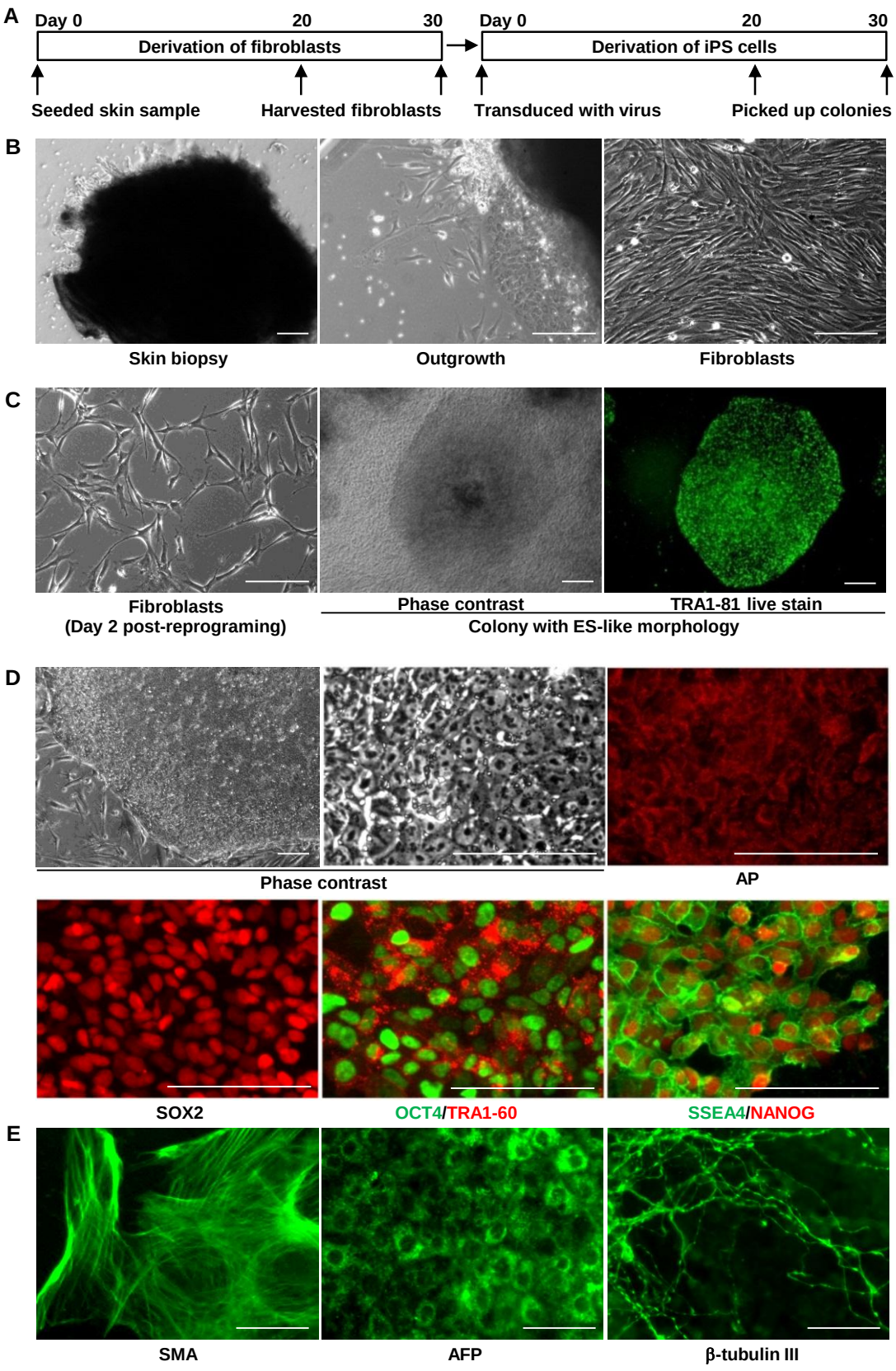
A
Day 0
20
30
Derivation of fibroblasts
Day 0
20
30
Derivation of iPS cells
Seeded skin sample
Harvested fibroblasts
Transduced with virus
Picked up colonies
B
Skin biopsy
Outgrowth
Fibroblasts
C
Fibroblasts
(Day 2 post-reprograming)
Phase contrast
TRA1-81 live stain
Colony with ES-like morphology
D
Phase contrast
AP
SOX2
OCT4/TRA1-60
SSEA4/NANOG
E
SMA
AFP
β-tubulin III

Figure S1. Derivation and Characterization of the Human iPSC Lines

(A) Schematic outlining of procedures/timing for derivation of human dermal fibroblasts (HDFs) and generation of iPSC lines.

(B) Serial morphological changes during HDF derivation. Shown from left to right are phase contrast images of a small skin piece minced from a skin biopsy, outgrown HDFs on day 4 post-explanting, and homogenous fibroblastic-like culture on day 14. Scale bar, 200 μm.

(C) Morphological changes during iPSC derivation. Shown from left to right are a phase contrast image of STEMCCA lentivirus-transduced HDFs one day after being transferred onto 6-well culture plates, a phase contrast image of an hESC-like colony on day 28 post-initial-transduction, and a fluorescent image of the same hESC-like colony live-stained with TRA1-81 (green). Scale bar, 200 μm.

(D) Verification of pluripotency of the undifferentiated iPSC line 903-20. Shown from left to right are (top panel) a phase contrast image of a colony showing up as tightly packed, homogeneous round, and with defined borders; a phase contrast image for the same colony at a higher magnification displaying high nucleus-to-cytoplasm ratio; and an immunofluorescent image demonstrating alkaline phosphatase activity (AP; red); and (bottom panel) immunofluorescent images for SOX2 (red), double-stained OCT4/TRA1-60 (green/red), and double-stained SSEA4/NANOG (green/red). Scale bar, 100 μm.

(E) *In vitro* differentiating potential of the undifferentiated iPSC line 903-20 toward different germ layers. Shown from left to right are immunofluorescent images of *in vitro* derived embryoid bodies (EBs) for the differentiation markers smooth muscle actin (SMA; the mesodermal lineage), α-fetal protein (AFP; the endodermal lineage), and β-tubulin III (the ectodermal lineage). Scale bar, 50 μm.

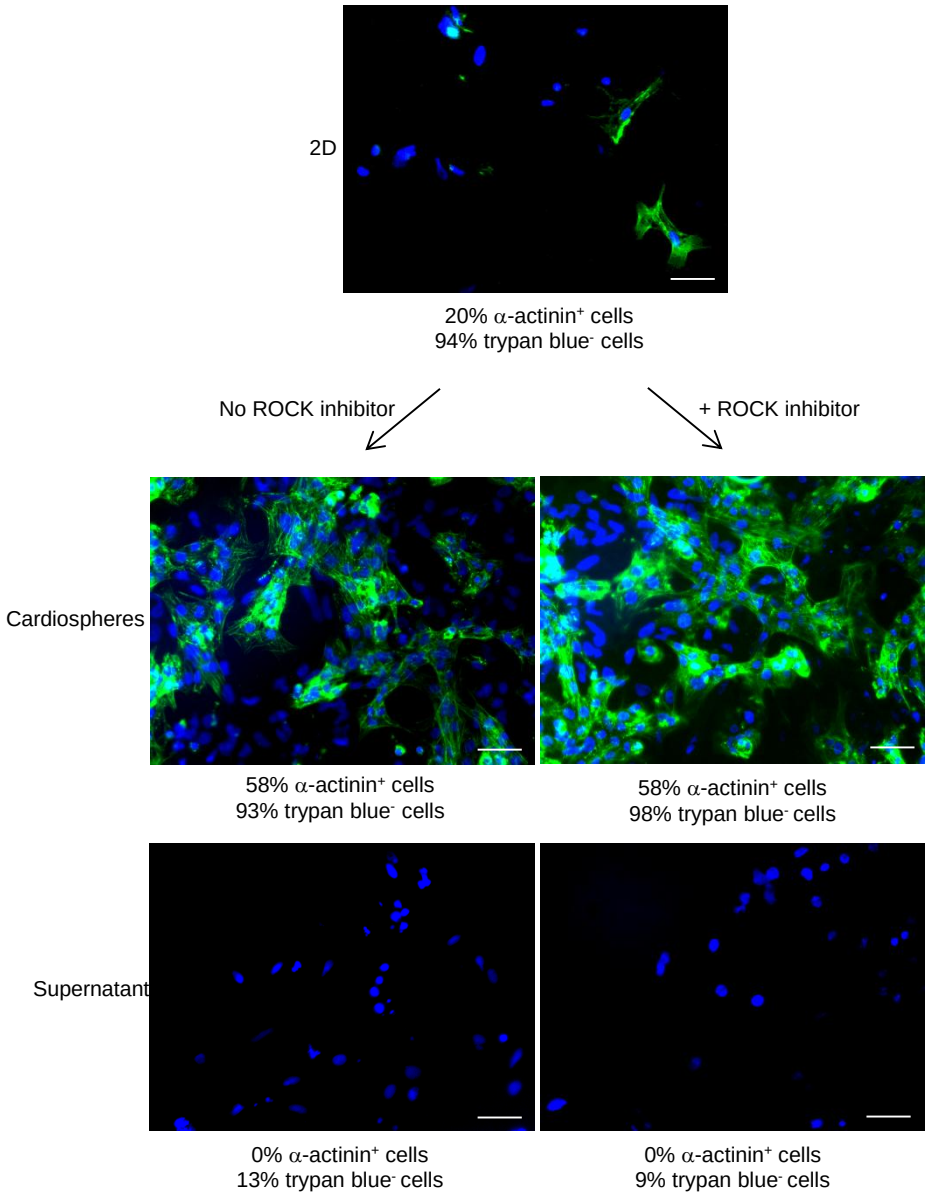

Figure S2. Characterization of Cell Viability and Enrichment of Cardiomyocytes during Cardiosphere Formation

2D differentiated cells derived from IMR90 iPSCs at day 23 were harvested, counted, and seeded into a microwell plate to form cardiospheres in medium with or without ROCK inhibitor (1 μM). After 24 hr, cardiospheres and supernatant were separated. The input 2D cells, cells from supernatant, and cardiospheres were dissociated, replated onto a gelatin-coated plate, and fixed the next day for immunocytochemical analysis of α-actinin. Cell viability was estimated by trypan blue exclusion. Scale bars, 50 μm.

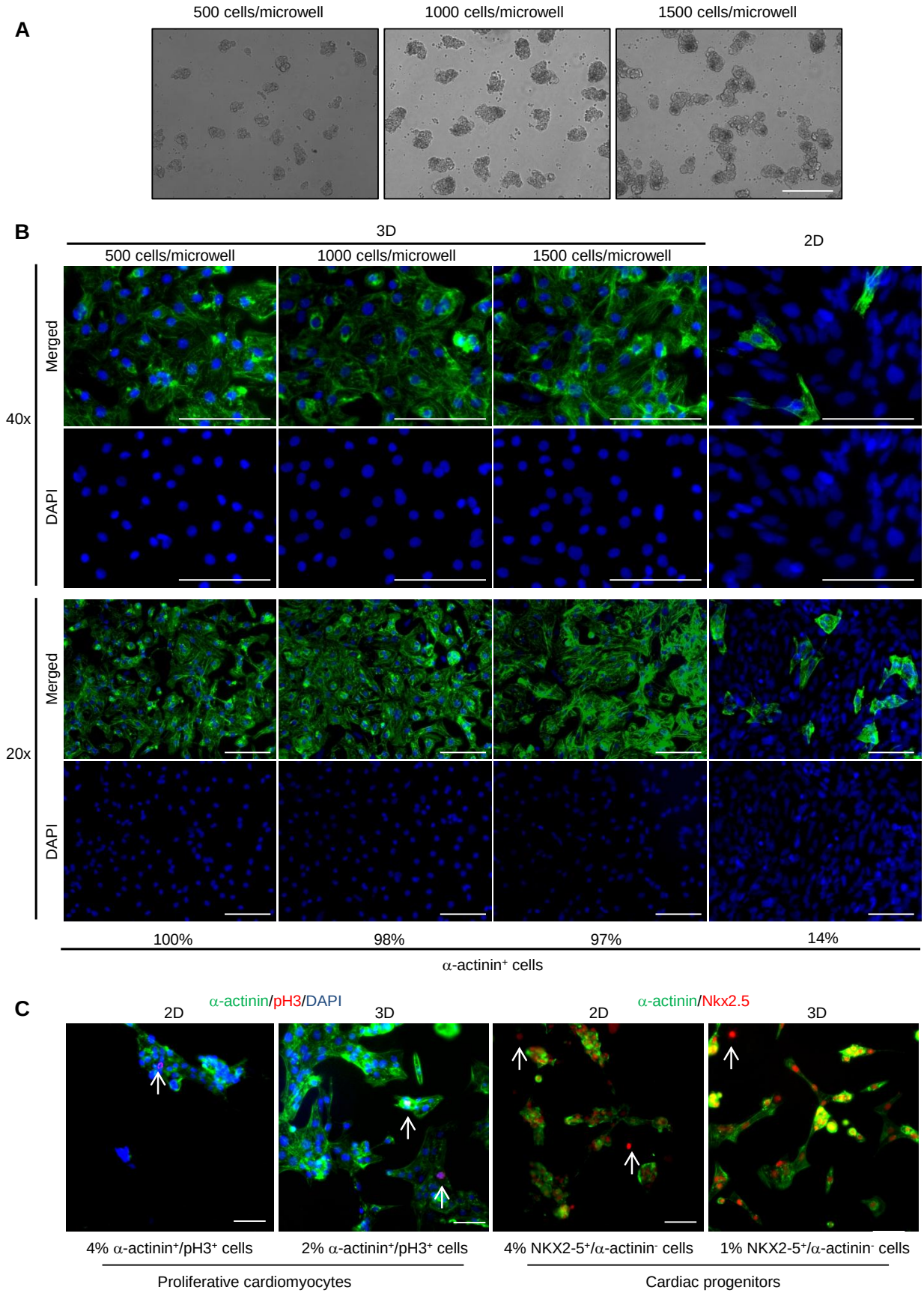
A
500 cells/microwell
1000 cells/microwell
1500 cells/microwell
B
3D
2D
500 cells/microwell
1000 cells/microwell
1500 cells/microwell
40x
Merged
DAPI
20x
Merged
DAPI
100%
98%
97%
14%
α-actinin+ cells
C
α-actinin/pH3/DAPI
α-actinin/Nkx2.5
2D
3D
2D
3D
4% α-actinin+/pH3+ cells
2% α-actinin+/pH3+ cells
4% NKX2-5+/α-actinin- cells
1% NKX2-5+/α-actinin- cells
Proliferative cardiomyocytes
Cardiac progenitors

Figure S3. Characterization of Enrichment of Cardiomyocytes by Cardiosphere Formation

(A) Effect of cell seeding densities on the formation of cardiospheres. The cardiospheres were generated using 2D differentiated culture derived from 903-20 iPSCs at day 14. Cardiospheres fromed in cultures using all 3 seeding densities (500, 1000, or 1500 cells/microwell). Images show morphology of 3D cardiospheres at day 14+4. Scale bars, 500 μm.

(B) Effect of cell seeding densities on the enrichment of cardiomyocytes. Input 2D cells at day 14 and 3D cardiospheres at day 14+7 were dissociated, replated, and fixed the next day before immunocytochemical analysis. α-actinin$^+$ cells consistently accounted for ~97-100% of the cardiosphere populations regardless of the input seeding cells harvested from the 2D population, in which the percentage of α-actinin$^+$ cell was ~14%. Immunocytochemical images were taken at magnifications of 20x and 40x, as indicated. Note: The robustness of cardiomyocyte enrichment was not dependent on the numbers of 2D input cells seeded for 3D cardiosphere formation. Scale bars, 100 μm.

(C) Detection of proliferative cardiomyocytes and cardiac progenitors. 2D differentiated cells derived from IMR90 iPSCs at day 17 were used to form cardiospheres. The input 2D cells, and dissociated cardiospheres at day 17+1 were seeded onto a gelatin-coated plate and fixed the next day for immunocytochemical analysis. Proliferative cardiomyocytes at M phase were detected by double staining of α-actinin (green) and pH3 (red). The cells were also costained with antibodies against NKX2-5 (red), a progenitor marker but persisting in cardiomyocytes, with α-actinin (green). Representative images of α-actinin$^+$/pH3$^+$ cells (proliferative cardiomyocytes) or NKX2-5 single positive cells (cardiac progenitors) are indicated by arrows. Scale bars, 50 μm.

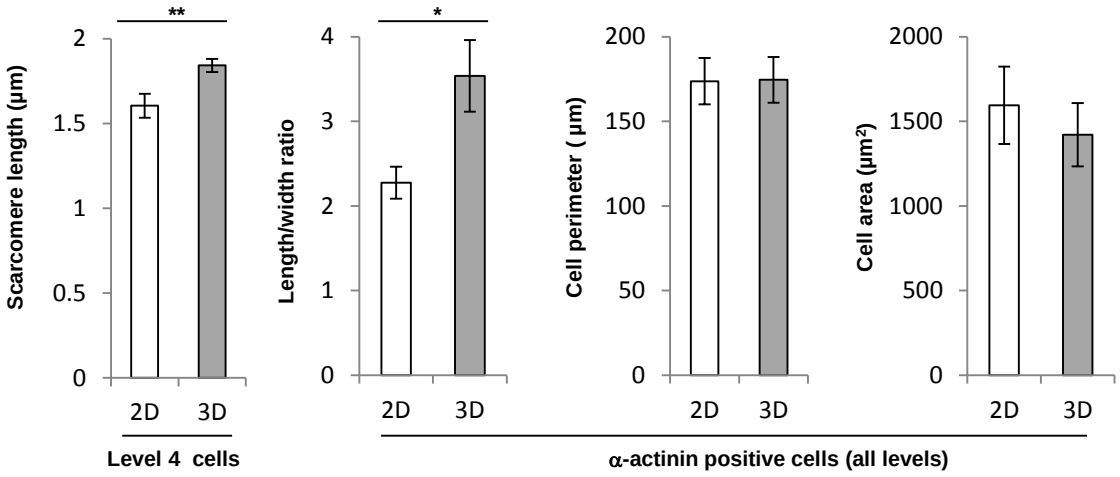

Figure S4. Measurements of Sarcomeric Lengths and Morphology of Cardiomyocytes
2D differentiated cells at day 14 were used to form cardiospheres. At day 14+7 or 14+8 cardiospheres and parallel 2D cultures were dissociated, replated, and fixed the next day for immunocytochemical analysis. Measurements were quantified in ImageJ software using images of α-actinin staining from n=21 to 34 cells per condition collected from cardiomyocytes derived from 903-20 or H7. Data are presented as mean±standard error. Statistical analysis was performed using a two-tailed Student's *t*-test in Microsoft Excel. *, p=0.01; **, p=0.005.

SUPPLEMENTAL EXPERIMENTAL PROCEDURES

Cells and Culture

Two iPSC lines, designated 903-20 and 903-19, were derived in this study (see below). Another iPSC line IMR90 (Yu et al., 2007) and an NIH-approved hESC line WA07 (H7) (NIHhESC-10-0061) (Thomson et al., 1998) were obtained from the WiCell Research Institute, Madison, WI. Undifferentiated hPSC lines were initially cultured on mouse embryonic fibroblast (MEF) feeders and then maintained under feeder-free condition as described (Xu et al., 2001). All culture media and reagents were purchased from Life Technologies, unless otherwise indicated. All cultures were maintained in 5% CO_2 at 37^{o}C.

In vitro Cardiomyocyte Differentiation

Guided *in vitro* cardiomyogenesis of undifferentiated hPSCs was achieved with growth factors (Laflamme et al., 2007) or small molecules (Lian et al., 2012) on adherent cultures as previously described with minor modifications. Briefly, confluent hPSCs were dissociated with Versene at 37°C for 5-7 min and subsequently re-plated onto Matrigel-coated plates (Corning) at a density of $1x10^5$ or $2x10^5$ cells per cm^2 in MEF-conditioned medium. The cells were fed daily with fresh MEF-conditioned medium containing 4-8 ng/mL human bFGF for 2 to 4 days until cells reached confluence and were then treated with growth factors or small molecules.

For cardiomyocyte induction by growth factors, cells were treated with 50-100 ng/mL recombinant human activin A (R&D Systems) in RPMI/B27-insulin-free medium (day 0). On day 1, the cells were maintained in RPMI/B27-insulin-free medium supplemented with 10 ng/mL recombinant human bone morphogenetic protein 4 (BMP4; R&D Systems). Four days later (i.e. on day 5), the medium was switched to RPMI/B27 and subsequently the cells were re-fed every alternative day with this medium until harvest.

For cardiomyocyte induction by small molecules, cells were treated with 12 μM CHIR99021 (Stemgent) in RPMI/B27-insulin-free medium (day 0) for 24 hr, subsequently incubated in RPMI/B27-insulin-free medium on day 1, followed by treatment on day 3 with 5 μM IWP4 (Stemgent), which was then removed on day 5 during the fresh RPMI/B27-insulin medium exchange. Subsequently, the medium was switched to RPMI/B27 on day 7 – and the cells were maintained in this medium, which was replenished every 2 days until harvest.

Histological analysis

Cardiospheres were fixed for 1 hr in 10% neutral buffered formalin and embedded in paraffin. Five micron sections were cut and adhered to SuperFrost Plus slides (VWR). Sections were stained with Hematoxylin and Eosin (VWR), Alcian Blue (Newcomers Supply), Fastgreen/Picrosirius Red (Sigma), and Masson's Trichrome (Sigma). All samples were imaged on a Nikon 80i microscope with a SpotFlex camera (Diagnostic Instruments).

Measurement of Intracellular Calcium Transient

Live cell imaging of intracellular calcium transients was used to assess functional characteristics of cardiomyocytes from cardiospheres that were generated from differentiated cultures at day 14. After 8 days in suspension culture, cardiospheres were re-cultured onto fibronectin or Matrigel-coated glass coverslips for additional 9 to 11 days. Coverslips containing cells were incubated with 5 μM of the calcium indicator dye Fluo-4 AM (Life Technologies) for 15 min at 37^{o}C, then transferred to a temperature-controlled microscope chamber and perfused at 37^{o}C with modified

Tyrode's solution (Wagner et al., 2005) (140 mM NaCl, 4 mM KCl, 2 mM $CaCl_2$, 1 mM $MgCl_2$, 10 mM HEPES, and 5 mM glucose, pH adjusted to 7.40 with NaOH). Optical recordings of intracellular calcium transients were acquired at 40x magnification using an inverted laser confocal scanning microscope Olympus FV1000 equipped with FluoView software (Olympus). These optical recordings were exported and analyzed with ClampFit 10.0 software (Molecular Devices). Data are presented as mean±standard error from 18 cardiosphere outgrowths.

Multielectrode Array (MEA) Recordings

Cardiomyocytes from cardiospheres were examined using a microelectrode array (MEA) data acquisition system, a 64 channel Muse MEA system (Axion Biosytems). Cardiospheres were dissociated with 0.25% trypsin/EDTA and $3x10^4$ cells were re-plated onto fibronectin-coated MEA chambers where they were maintained in RPMI-B27 medium. Cells were allotted 8 days to stabilize prior to being subjected to the recording. Extracellular recording was performed using the MEA system for 60 s at baseline and at 5 min after drug application. β-adrenergic agonist isoproterenol (isoproterenol hydrochloride; Sigma) was added to the MEA chamber at a final concentration of 10 nM. The data were analyzed using the AxIS software.

Immunocytochemical Analysis

Immunocytochemical analysis was carried out to assess the pluripotency and the *in vitro* differentiating capacity of iPSCs (i.e. EB formation and sequential three-germ-layer differentiation) as well as the proportion and the *in vitro* phenotypes of cardiomyocytes.

In brief, beating monolayer cultures, cardiospheres, and cells in supernatant were dissociated with 0.25% trypsin/EDTA and re-plated at a density of $2\text{-}5x10^4$ cells/well on 0.5% gelatin-coated 96-well culture plates (Nalgene Nunc International) and cultured for 1 day before processed for fixation. Cell preparations (undifferentiated iPSCs, EB outgrowths, or cells from the dissociated contracting monolayer,cardiospheres and cells in supernatant) were washed with cold PBS and fixed with 2% or 4% (vol/vol) paraformaldehyde (Sigma) for 10-15 min at room temperature (RT), permeabilized with 100% ethanol (Sigma) for 5 min, blocked with 5% (vol/vol; diluted in PBS) normal goat serum (NGS) overnight at 4^oC, and then incubated for 2 hr at RT on a rotator with appropriate primary antibodies (Abs) of optimal concentrations diluted in PBS plus 5% NGS. The preparations were subsequently rinsed three times with cold PBS for 5-10 min – with gentle shaking – to remove unbound Abs prior to being labeled with conjugated secondary Abs of optimal concentrations diluted in the same solution as the primary Abs for 1 hr at RT in the dark, followed by being washed three more times in cold PBS for 5-10 min – with gentle shaking. Cell nuclei were counterstained for visualization with 4′,6-diamidino-2-phenylindole (DAPI, or Vectorshield, Vector Laboratories), following the manufacturer's instructions. The stained cell immunocomplexes were sequentially subjected to imaging and morphological analysis under fluorescence microscopy, as described below.

For whole mount immunostaining of 3D cardiospheres, cell aggregates were fixed in 4% paraformaldehyde for 1 hr, rinsed 3 times with 1.5% normal donkey serum (NDS), permeabilized for 30 min in 1.5% Triton-X 100, re-fixed in 4% paraformaldehyde for 15 min, blocked for 3 hr in 1.5% NDS, and then incubated overnight at $4^{\circ}C$ in appropriate primary Abs. The cardiospheres were subsequently rinsed 3 times in 1.5% NDS, incubated in the appropriate secondary Abs for 4 hr, rinsed 3 times in 1.5% NDS, and counterstained with Hoechst for 15 min. Samples were stored in PBS until imaging.

The primary Abs utilized included those that target: i) hPSC pluripotent markers, such as endogenous OCT4, SOX2, NANOG, SSEA-4, TRA-1-60, and TRA-1-81; ii) three-germ-layer markers, such as endodermal marker α-fetoprotein, mesodermal marker smooth muscle actin, and ectodermal marker β-tubulin III; and iii) cardiomyocyte-associated markers, such as sarcomeric α-actinin (the cytoskeleton binding protein), cardiac troponin-I (cTnI), sarcomeric myosin heavy chain (sMHC, the major contractile protein), and connexin-43 (Cx43; the gap junctions between neighboring cells). Information about primary and secondary Abs, including their source, property, application and dilution, is shown in Table S1.

Phase-contrast and Fluorescence Photomicroscopy/imaging

Phase-contrast and fluorescent images for cultured (unstained) and stained hPSCs, cardiomyocytes, and HDFs were routinely visualized using a Zeiss Axio Vert.A1 phase contrast and fluorescence inverted microscope (Zeiss), which was equipped with a Zeiss AxioCam digital camera system for micro-photographing. Captured/acquired images were processed and exported using Zeiss AxioVision LE imaging software and image analysis and quantification were performed in Adobe Photoshop (Adobe Systems). Cells were visualized for size, area, and sarcomeric content/organization. Percentages of cardiomyocytes (α-actinin$^+$ cells), cardiac progenitors (NKX2-5$^+$/α-actinin$^-$ cells) and proliferative cardiomyocytes (α-actinin$^+$/pH3$^+$ cells) based on immunocytochemical analysis were obtained by counting n=214 to 896 cells per condition. Measurement of sarcomeric lengths, cell areas, cell perimeters and ratios of length and width was quantified using images of α-actinin staining from n=21 to 34 cells per condition in ImageJ software. Phase images of cardiospheres were acquired using an EVOS FL system or a Zeiss Axio Vert.A1 phase contrast microscope. Fluorescence confocal imaging of cardiospheres was acquired with a Zeiss LSM700-405. Images were processed with the Zeiss ZEN 2011 software.

Statistics

Data are presented as mean+standard error or standard deviation as indicated in each figure legend. Standard deviation was used to determine how much variation was observed in sizes of cardiospheres and in qRT-PCR analysis within a given experiment. Standard error was used to indicate the uncertainty around the estimate of the mean of calcium measurement, sarcomeric length and cell morphology measurement. Statistical analysis of sarcomeric lengths and cell morphology was performed using a two-tailed Student's t-test in Microsoft Excel.

Flow Cytometric Analysis of Sarcomeric α-actinin

Cardiomyocyte purity of the 2D and 3D cultures was quantitatively assessed by flow cytometric analysis for the intracellular cardiomyocyte-associated protein, sarcomeric α-actinin, as previously described (Xu et al., 2011). Briefly, the differentiated cells were detached from cultures and individualized by incubation with 0.25% trypsin/ EDTA at 37°C for 5-7 min. Remaining cell aggregates were gently disrupted/dispersed by cautiously pipetting up and down. Prior to fixation, cells (4-7x10^5 cells) were first incubated on ice in the dark for 15 min with a dye for detection of dead cells, ethidium monoazide (EMA), washed twice with staining buffer (SB; PBS plus 2% (vol/vol) heat inactivated fetal bovine serum), and sequentially exposed to bright light for 10 min at RT. The resultant singly-dissociated cell preparations were subsequently fixed with 4% (vol/vol) paraformaldehyde for 30 min at RT, followed by permeabilization of cell membranes in ice-cold methanol. Permeabilized cells were then blocked

for nonspecific binding with blocking buffer (BB), which was made up of SB supplemented with 20% (vol/vol) NGS. Subsequently, blocked cells were stained with either a mouse sarcomeric α-actinin monoclonal Ab or an appropriate matching isotype control (mouse IgG1), for 20 min at RT. Following primary Ab and matching isotype staining, cells were washed in SB and were then incubated with the secondary Ab goat anti-mouse IgG1 conjugated to FITC for 20 min at RT in the dark. Stained cell samples were then washed three times with SB prior to being re-suspended in 200-300 µl SB for acquisition. Information about the primary and secondary Abs, including their source, property, application, and working concentration, is shown in Table S1.

Data were acquired using a FACSCanto II flow cytometer (Becton-Dickinson Biosciences) utilizing the FACSDiva 6 software and with at least 10^4 EMA-negative events collected. Positive staining was defined as the fluorescence emission levels exceeding those obtained by ~99% of cells stained with the matching IgG isotype control. Dot plots quantifying the percentage of live, α-actinin-positive or isotype control cells were generated as FCS Express file using the FACSDiva 6 software (Becton-Dickinson Biosciences). Data were analyzed offline using FlowJo software (Treestar). All cells were gated according to light scatter and fluorescence (FITC and PerCy5), bandpass filter 530/30-A and 670LP-A, respectively parameters.

Flow Cytometric Analysis of Cell Viability by Annexin V and Propidium Iodide (PI)

After 24 hr in an AggreWell™ plate (day 14+1), cardiospheres were gently harvested and transferred to a 15 mL conical tube. The tube was held vertically for 30-60 sec, or until spheres settled to the bottom. Careful not to disturb the spheres, the supernatant was removed using a pipette and transferred to a separate tube. Both the cardiosphere and supernatant fractions were each transferred into flat, ultra-low-adhesion dishes for phase-contrast imaging. After imaging, both fractions were returned to their respective tubes and dissociated for 3 min with 25% Trypsin/EDTA. Tubes were subsequently spun for 5 min at 200×g and resuspended for cell counting. Approximately $2.5x10^5$ cells were aliquoted per tube for flow cytometry. The FITC Annexin V/PI Dead Cell Apoptosis Kit for Flow Cytometry (Invitrogen) was used to stain the samples according to the manufacturer's instructions. Data shown were acquired on the BD FACSCanto™II flow cytometer using BD FACSDiva™ software. PI florescence was plotted against Annexin V fluorescence. The upper right quadrant ($Annexin^+/PI^+$) depicts necrotic cells; lower right ($Annexin^+/PI^-$), apoptotic cells; and lower left ($Annexin^-/PI^-$), live cells.

Cell Aggregation Inhibition Assays

Cell aggregation inhibition assays were performed similarly as described (Puch et al., 2001) using 903-19 iPSC and H7 cell-originated cardiomyocyte populations. Freshly isolated or cryopreserved cells harvested by 0.25% trypsin/EDTA from monolayer cultures at days 14 to 29 of differentiation were plated onto flat wells of 96-well plates at a density of $4.4x10^4$ cells (in 50 µl medium) per well for immediate photomicroscopy. The cells were then transferred – at 1:1 (well:well) ratio – to U-shaped wells of low attachment 96-well plate (to facilitate cell aggregation) containing pre-warmed RPMI/B27 medium with N-cadherin, NCAM-1 (CD56), or isotype control Abs at a concentration of 80 or 160 µg/ml (in 50 µl medium per well). The plates were incubated in a 5% CO_2 air environment at 37°C. Four hours later, cell aggregation was observed under microscope at U-shaped wells prior to being transferred to flat wells at 1:1 (well:well) ratio for confirmation of cell aggregate appearance. Photomicroscopy was carried out at this time point on both types of wells. Each test condition was completed in duplicate

wells. Five independent experiments (two with H7 cells and three with 903-19 iPSCs) were conducted. Antibodies for these assays were all supplied in a sterile solution and suitable for cell culture; details are listed in Table S1. Please note that the antibody against N-cadherin has been shown to be capable of inhibiting adherent junction formation (Puch et al., 2001).

Derivation of Human iPSC Lines

Procedures involved in human tissue collection and processing to derive iPSC lines were carried out in accordance with and approved by the Institutional Review Board of Emory University and Children's Healthcare of Atlanta. The iPSC lines were created through delivery into human dermal fibroblasts (HDFs) with mouse reprogramming factors *Oct4*, *Klf4*, *Sox2*, and *c-Myc* that were co-expressed by a single polycystronic lentiviral vector "stem cell cassette", or STEMCCA (Sommer et al., 2009). The lentivirus particles were produced via triple transient transfection of low-passaged human embryonic kidney (HEK) 293T cells with the STEMCCA cassette, the Gag-Pol psPAX2 expression packaging plasmid, and the VSV.G pMD2.G envelope expression helper plasmid. Supernatant containing pseudoviral particles was harvested and clarified by low-speed centrifugation and filtering, followed by being concentrated through ultracentrifugation. Concentrated virus was subsequently re-suspended and tittered based on its p24 content using the HIV-1 p24 antigen capture ELISA.

For HDF derivation, a skin biopsy was obtained from an African-American two-month old male undergoing gastroesophageal reflux repair surgery, was minced into small pieces and cultured under glass coverslips using MEF medium supplemented with Amphotericin B (an antimycotic compound; 2.5 µg/mL). Outgrown HDFs were sequentially isolated using 0.25% trypsin/EDTA and passaged (passage 1) at high cell density (~10^5 cells/cm^2) onto T25 culture flasks. Cells were subsequently kept expanded at regular density (~10^4 cells/cm^2) whenever they reached 80-90% confluence – and until they became homogenous fibroblastic-like cultures.

For reprogramming, singly-dissociated HDF cells were plated onto a 6-well culture plates at a density of $5x10^4$/well and transduced – the next day upon medium dilution – with the STEMCCA virus either at MOI of 1, 5, 10, or 25, diluted in 6 µg/ml polybrene (Sigma)-contained MEF medium. Cells were re-transduced on the following day using the same condition. One day later, cells were transferred onto 6-well culture plates coated with Matrigel (Becton-Dickinson Biosciences) (diluted 1:60 in DMEM/F12 medium) and were subsequently maintained in MEF conditioned medium supplemented with 8 ng/ml bFGF, which was replenished daily onwards until colony selection. Human embryonic stem cell (hESC)-like colonies were typically observed on days 15-24 post-initial-transduction. Based on hESC-like morphology and live-stained positivity with TRA1-81, putative iPSC colonies were then mechanically dissected under microscope and re-plated on a fresh irradiated MEF-feeder layer (at a density of one single colony per well). These hESC-like colonies were continuously cultured as undifferentiated hPSC cells using previously described procedures (see above), and the lines with stable hESC-like morphology were feeder-free propagated for further experiments.

The pluripotency of the undifferentiated lines was verified by the expression of pluripotency markers and *in vitro* differentiating capacity. Expression of specific hPSC markers was examined by ICC staining (see above), and alkaline phosphatase activity was assayed using VECTOR Red Alkaline Phosphatase Substrate Kit (Vector Laboratories). The general *in vitro* differentiating capacity was determined using the EB formation method. In brief, 70-80%-confluent undifferentiated cultures were enzymatically detached from Matrigel-coated cultured plate using pre-warmed collagenase IV (200 U/ml) for 5-7 min at 37^0C. Colonies were then

harvested as cell clusters and transferred into ultralow-attachment plates (Corning Inc., Corning, NY) for the formation of aggregates (EB) in suspension using differentiation medium (DM), which is composed of 80% KO DMEM, 20% FBS, 1 mM L-glutamine, 0.1 mM β-mercaptoethanol, and 1% non-essential amino acid (all from Life Technologies, unless otherwise indicated). DM was exchanged on day 2, and formed EBs were re-plated on 0.5% gelatin-coated 96-well plate on day 4. The attached EBs were maintained in DM, which was sequentially exchanged every alternative day onwards – until day 14 when cells were fixed with 2% paraformaldehyde. Fixed cells were subjected to ICC staining, as described above, for assessment of three germ layer specific markers, including α-smooth muscle actin (SMA; a mesodermal marker), α-fetal protein (AFP; an endodermal marker), and β-tubulin III (an ectodermal marker).

SUPPLEMENTAL REFERENCES

Laflamme, M.A., Chen, K.Y., Naumova, A.V., Muskheli, V., Fugate, J.A., Dupras, S.K., Reinecke, H., Xu, C., Hassanipour, M., Police, S., *et al.* (2007). Cardiomyocytes derived from human embryonic stem cells in pro-survival factors enhance function of infarcted rat hearts. Nat Biotechnol *25*, 1015-1024.

Lian, X., Hsiao, C., Wilson, G., Zhu, K., Hazeltine, L.B., Azarin, S.M., Raval, K.K., Zhang, J., Kamp, T.J., and Palecek, S.P. (2012). Robust cardiomyocyte differentiation from human pluripotent stem cells via temporal modulation of canonical Wnt signaling. Proc Natl Acad Sci U S A *109*, E1848-1857.

Puch, S., Armeanu, S., Kibler, C., Johnson, K.R., Muller, C.A., Wheelock, M.J., and Klein, G. (2001). N-cadherin is developmentally regulated and functionally involved in early hematopoietic cell differentiation. J Cell Sci *114*, 1567-1577.

Sommer, C.A., Stadtfeld, M., Murphy, G.J., Hochedlinger, K., Kotton, D.N., and Mostoslavsky, G. (2009). Induced pluripotent stem cell generation using a single lentiviral stem cell cassette. Stem Cells *27*, 543-549.

Thomson, J.A., Itskovitz-Eldor, J., Shapiro, S.S., Waknitz, M.A., Swiergiel, J.J., Marshall, V.S., and Jones, J.M. (1998). Embryonic stem cell lines derived from human blastocysts. Science *282*, 1145-1147.

Wagner, M.B., Wang, Y., Kumar, R., Tipparaju, S.M., and Joyner, R.W. (2005). Calcium transients in infant human atrial myocytes. Pediatr Res *57*, 28-34.

Xu, C., Inokuma, M.S., Denham, J., Golds, K., Kundu, P., Gold, J.D., and Carpenter, M.K. (2001). Feeder-free growth of undifferentiated human embryonic stem cells. Nature Biotech *19*, 971-974.

Xu, C., Police, S., Hassanipour, M., Li, Y., Chen, Y., Priest, C., O'Sullivan, C., Laflamme, M.A., Zhu, W.Z., Van Biber, B., *et al.* (2011). Efficient generation and cryopreservation of cardiomyocytes derived from human embryonic stem cells. Regen Med *6*, 53-66.

Yu, J., Vodyanik, M.A., Smuga-Otto, K., Antosiewicz-Bourget, J., Frane, J.L., Tian, S., Nie, J., Jonsdottir, G.A., Ruotti, V., Stewart, R., *et al.* (2007). Induced pluripotent stem cell lines derived from human somatic cells. Science *318*, 1917-1920.

Table S1. Antibodies

Type	Subject (Application)	Antibody target	Origin /isotype	Supplier	Catalog number	Dilution or concentration
Primary	iPSCs (ICC or AS)	NANOG	Rabbit IgG	EMD Millipore	AB9220	1:200
		OCT4	Mouse IgG_1	EMD Millipore	MAB4401	1:1,000
		SSEA-4	Mouse IgG_3	DSHB	MC-813-70	1:200
		SOX2	Rabbit IgG	Biolegend	630801	1:200
		TRA 1-60 (AS)	Mouse IgM	Stemgent	09-0068	1:500
		TRA 1-81 (AS)	Mouse IgM	Stemgent	09-0069	1:500
		TRA 1-60 (ICC)	Mouse IgM	EMD Millipore	MAB4360	1:200
		TRA 1-81 (ICC)	Mouse IgM	EMD Millipore	MAB4381	1:200
	EB (ICC)	Alpha fetoprotein	Mouse IgG_1	Life Technologies	18-0003	1:100
		α-Smooth muscle	Mouse IgG_{2a}	Sigma	A5228	1:400
		β-Tubulin III	Mouse IgG_{2b}	Sigma	T5076	1:400
	Cardiomyocytes (ICC)	α-actinin	Mouse IgG_1	Sigma	A7811	4 ug/ml or 1:800
		Connexin 43	Rabbit IgG	Sigma	C6219	1:400
		MF20 (sMHC)	Mouse IgG_{2b}	DSHB	MF 20-c	1:200
		NKX2-5	Rabbit IgG	Santa Cruz Biotech	sc-14033	1:400
		Troponin I	Mouse IgG_{2b}	EMD Millipore	MAB1691	1:200
		pH3	Rabbit IgG	EMD Millipore	06-570	1:500
	Cardiomyocytes (FCM)	α-actinin	Mouse IgG_1	Sigma	A7811	4 µg/ml
		Isotype control	Mouse IgG_1	BD Biosciences	554121	4 µg/ml
	Cardiomyocytes (AI)	NCAM-1 (CD56)	Mouse IgG_1	Biolegend	318324	40 or 80 µg/ml
		Isotype Control	Mouse IgG_1	Biolegend	401403	40 or 80 µg/ml
		N-cadherin	Mouse IgG_1	Sigma	C3865	40 or 80 µg/ml
Secondary	ICC FCM	Alexa 488, Goat anti-mouse IgG_1		Life Technologies	A-21121	1: 400 or 1:1000
		Alexa 488, Goat anti-mouse IgG_3		Life Technologies	A-21151	1:200
		Alexa 488, Goat anti-mouse, IgM		Life Technologies	A-21042	1:200
		Alexa 594, Goat anti-rabbit IgG		Life Technologies	A-11012	1: 400 or 1:1000
		Alexa 594, Goat anti-mouse IgG_{2b}		Life Technologies	A-21145	1:1000
		FITC, Goat anti-mouse IgG		Sigma	F2012	1:120

Abbreviations: AI, aggregation inhibition; AS, alive staining; CMs, cardiomyocytes; DSHB, Developmental Studies Hybridoma Bank; EB, embryoid bodies; FCM, flow cytometry; ICC, immunocytochemistry; iPSCs, induced pluripotent stem cells